New Prospects of Optical Wireless Communication Systems Exploiting VCSEL-based Transmitters

L. Gilli *Member, IEEE*, G. Cossu *Member, IEEE* and E. Ciaramella *Senior Member, IEEE*

***Abstract*—In the last decades, Vertical Cavity Surface Emitting Lasers (VCSELs) emerged as a dominant technology for short-reach high-data rate networks thanks to several advantageous features. These include low power consumption, high modulation speeds, low costs, and compact size. More recently, these inherent characteristics of the VCSELs have also made them exceptionally suited for a variety of Optical Wireless Communication (OWC) applications, particularly for short-distance links, up to a few meters.**

This paper reviews a range of new and promising applications for VCSELs within emerging OWC domains: Data Centers (DCs), space, and harsh environment. We present and discuss different VCSEL-based OWC systems that were designed, implemented, and tested in these emerging scenarios. For the DCs scenario, we present a novel approach to establish OWC links able to reach data rates up to 40 Gbit/s with a single VCSEL. In the space environment, innovative OWC systems can support data communication among electronic elements placed in line-of-sight outside the spacecraft or inside a small satellite. VCSELs can be also exploited for data transmission in the very harsh environment of high-energy physics experiments. Here, a 10 Gbit/s OWC system was designed for the Board-to-Board (B2B) link in High Energy Physics (HEP) experiments.

Since space and HEP applications exhibit extreme conditions, the OWC systems and, particularly, the VCSELs were tested to assess their behavior under strong mechanical, thermal, and radiation stress.

***Keywords*—Free-space optics, Wireless communication, Vertical cavity surface emitting, Data-center network**

I. Introduction

In the near future, Optical Wireless Communication (OWC) will be a key valuable addition in various wireless communication areas. Currently, there is a growing interest in exploring OWC as a powerful complementary technology to Radio Frequency (RF) wireless and traditional cabled systems [1], [2]. As in RF, OWC systems can be very different in terms of data rate, user mobility, transmission distance, involved devices, link architecture, and specific optical properties of the operational environment [3]–[6]. This is graphically sketched in Fig. 1: RF technologies are well-known, and it is obvious that each of them corresponds to specific hardware. The same applies for OWC, where different transmitters, receivers, and link configurations can be considered, depending on data rate, coverage area, and distance. Three main classes of OWC configurations are usually considered [4]: the first is Non Line-of-Sight (N-LOS), where the light from the source has a significant divergence angle, illuminating the whole environment; the scattering and reflections ensure that the receiver always collects enough signal, albeit with limited bit rates. Conversely, Directed Line-of-Sight (D-LOS) uses beams with small divergence and clear Line-of-Sight (LOS), thus is can achieve high bit rates but requires an accurate alignment. Lastly, as an intermediate condition, Non-Directed Line-of-Sight (ND-LOS) architecture requires line-of-sight, but it offers a larger coverage area by leveraging wide beam emission.

Light Emitting Diode (LED) are usually employed for N-LOS and ND-LOS links because those scenarios require diffuse links, high user mobility, lower data rate transmissions. These configurations were proposed for indoor applications in home and office [7]–[9] and, recently, for onboard satellites [6], [10].

On the other hand, Vertical Cavity Surface Emitting Lasers (VCSELs) can be the optimal choice in the D-LOS links. In this case, the optical systems are characterized by a high modulation bandwidth, low divergence, and low power consumption [11]–[13]. Indeed, initially used in data storage and retrieval, such as in CDs and DVDs, VCSELs were also largely exploited for data communication, supporting fiber connections up to 300 m [14] and making them suitable for data-center applications. Projections indicate that VCSEL revenues for data communication are expected to exceed 2 billion USD in 2027 [15], [16]. In the last few years, the bandwidth of the VCSELs emitting at 850 nm increased from 23 GHz [17] to over 30 GHz [18]. Various groups reported bit rates exceeding 40 Gbit/s using VCSELs emitting at different wavelengths [19], [20]. This increase in bandwidth allowed for the implementation of VCSEL-based short-links with line rates of 56 Gbit/s using Pulse-Amplitude Modulation (PAM) at 28 Gbaud, recently increased up to 112 Gbit/s in the 800 GbE transceivers (TRXs) [21], [22], and even up to 200 Gbit/s per line [23].

More recently, VCSEL devices were exploited in new wireless applications, reporting impressive results. In this paper, we report some research demonstrations of OWC systems based on VCSELs that were recently obtained. They refer to various types of applications: Board-to-Board (B2B) links in Data Centers (DCs), in spacecraft, and for High Energy Physics (HEP) data communications. These are quite new, and they are very different, so they still have to be deeply explored, leaving the way open for relevant innovations in the OWC domain.

The paper is structured as follows. In Section II, we recall shortly the key characteristics of the VCSELs. Section III describes OWC systems designed for DC applications. The

L. Gilli, G. Cossu and E. Ciaramella are with Scuola Superiore Sant'Anna, Via Moruzzi 1, 56124 Pisa, Italy.e-mail: g.cossu@santannapisa.it.

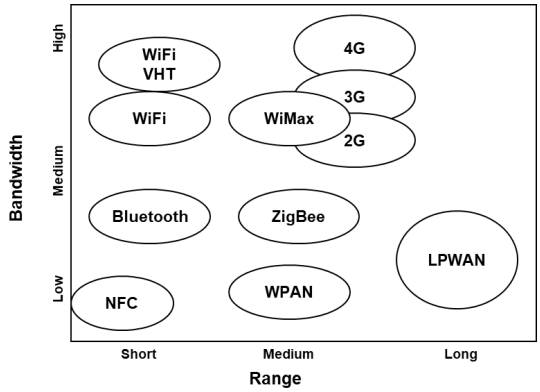

(a)

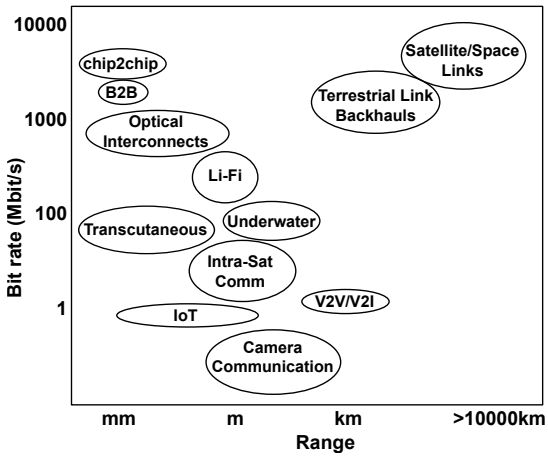

(b)

Fig. 1: Families of most common and popular RF (a) and OWC technologies (b).

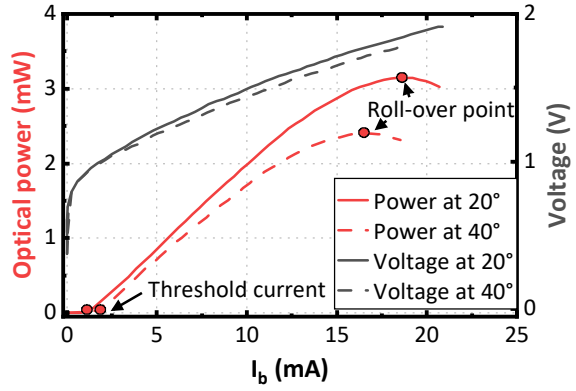

Fig. 2: Typical LIV curve as a function of two temperature values

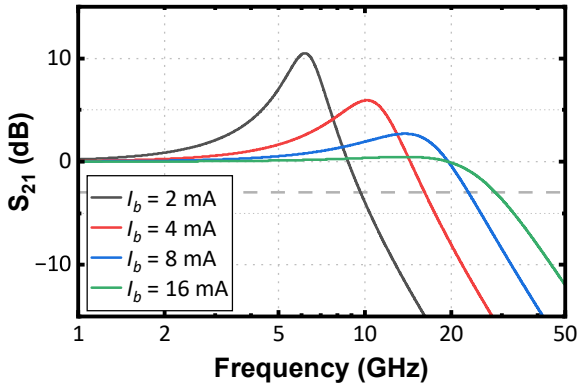

Fig. 3: Typical S_{21} curve of a VCSEL at different bias currents.

results of using VCSELs in harsh environments like space and HEP are presented in Section IV. Lastly, in Section V, we conclude.

II. VCSEL PROPERTIES

VCSELs are a class of lasers in which the direction of the emission of the radiation is normal to the top surface. The VCSEL technology was first demonstrated in [24], [25] and since then they were extensively described [26]–[29]. Here, we summarize the key features. A typical VCSEL includes an active region composed of quantum wells confined by distributed Bragg reflectors on top and bottom, made by epitaxial or dielectric materials. The cavity is oriented vertically, perpendicular to the substrate and aligned to the active area. Both static and dynamic responses are critical for studying and modeling the VCSEL performance.

The static measurements involve varying the bias current I_b and measuring the voltage V and the optical output power P_{out} of the VCSEL, referred to as Light-Current-Voltage (LIV) curve. From a typical LIV curve, shown in Fig. 2, we can observe the low threshold current (typically a few mA) and the slope efficiency, which indicates how P_{out} increases with I_b after the threshold. Additionally, we can see the roll-over point, where the maximum P_{out} is achieved, and any further increase in I_b results in a reduction in the emitted power, due to thermal effects. All these factors are influenced by the temperature, which is a key parameter to consider in the link design.

As for other semiconductor lasers, the electrical bandwidth of the VCSELs can reach values of tens of GHz. The modulation speed is limited by the intrinsic damping of the resonant carrier-photon interaction [30], and by the effect of self-heating and parasitic capacitors, typically given by [31], [32]

$$H(f) = \frac{f_r^2}{f_r^2 - f^2 + i\gamma f/2\pi} \tag{1}$$

where f_r and γ represent the resonance frequency and the damping rate, respectively. f_r typically rises with the bias current. This can be seen from Fig. 3, where we report the typical S_{21} curve of a VCSEL for different bias current values.

The specific geometry of the VCSELs makes them smaller than other semiconductor lasers allowing for integrating these devices on electronic circuits or implementing multi-laser arrays [28]. The typical linewidth is very narrow (order of tens of pm). Linewidth limitations can occur in systems using coherent detection or phase modulation. However, the systems

in this work exploit Intensity Modulation with direct detection (IM/DD), where these issues can be neglected.

Mostly, they have circular beams with limited divergence ($\sim 10°$) and the large modulation bandwidth allows for high-speed transmitters (TXs) with direct modulation, which are apparently very compact. Hence, VCSELs are particularly suited in D-LOS configurations, where we need a quite accurate alignment, high data rate, and limited size. This link architecture does not rely on scattering and diffuse links as for ND-LOS configurations. Indeed, in D-LOS the used TXs produce a beam with limited divergence angle, making them robust to multipath effects. The robustness is further enhanced by receivers (RXs) that have a low Field-of-View (FoV)

VCSELs can cover a wide range of wavelengths, from the near Infrared (IR) up to 1550 nm. For generic use in OWC, no wavelength has a significant advantage over the others, so the choice of a particular source can depend on the specific details of the application scenario. As an example, the presence of other strong light sources may cause interference, but this can be eliminated by selecting a TX-RX pair operating in a different spectral range (suitable for OWC transmission). In other cases, the operating wavelength can be chosen depending on the available devices that meet the requested bandwidth.

Although VCSELs are produced both as single-mode and multi-mode, all systems in this paper use single-mode VCSELs since these are better suited to the requirements of free space communications. Multi-mode VCSELs could have a smaller divergence angle than single-mode, but they have a rather irregular transversal intensity distribution (sometimes even with a minimum intensity on-axis). On the other hand, single-mode VCSELs have an almost Gaussian emission pattern, which makes it easier to align them with the center of the photodetector and maximize the collected optical power.

They also present a few drawbacks for OWC applications; mostly, the divergence of the beam is low yet not negligible: this can be corrected by a (micro) lens, making the TX more complex. Moreover, the available optical power is quite low (typically, few mW), which could limit the final distance. To address this issue, high-power VCSEL arrays were recently produced [33], with up to 200 mW output power.

VCSELs are also very safe to use. As known, the safety level of a LASER source is defined in the European standard IEC60825-1: "Safety of laser products" [34] and depends on the wavelength, the emission angle, the emitted optical power, the distance of the user from the source, and the time exposure to the source. Specifically, all the VCSELs employed in these experiments are Class 1M LASER sources: assuming an exposure time of 1 s, the shortest safe distance is not greater than 5 cm in all cases.

In summary, the small size, in addition to the low production costs, the low power consumption, and the wide electrical bandwidth, make the VCSEL an excellent candidate for new OWC systems.

III. OWC System for Data Centers

A first scenario that can benefit from using VCSEL-based OWC systems is the high-speed data transmission in DCs. The complexity and size of DCs are increasing exponentially: performance, power consumption, cabling, maintenance, and flexibility will be key issues in the future intra-DC networks. Today, these networks are made of optical fibers connecting Top-of-Rack (ToR) switches: using fibers, these networks have limitations in scalability, reconfiguration, and cooling efficiency. In those fiber links, VCSELs are used largely, often combined with multi-mode fibers. The fiber-based connections present severe issues, such as space occupancy, fan obstruction, maintenance and reconfigurability. These can be overcome by means of wireless alternatives to obtain communication systems that are easily reconfigurable and with better cooling efficiency. Noteworthy, RF cannot provide the speed values of OWC. Moreover, RF signals spread around, whilst optical beams can have very high directivity; thus optical signals can support much higher values of user density, e.g. density of TX/RXs. Since wireless RF systems cannot achieve neither the data rates nor the user density, OWC technology represents the only promising alternative to cabled lines. Moving VCSELs from fibers to wireless might look straightforward, but it is not: indeed, it requires a complete redesign of the link and a careful selection of devices. Clearly, the goal is to achieve data rates that are comparable to those in a DC with a marked reduction of occupied volume and, hopefully, of power consumption.

For this application, we first realized and demonstrated a 10 Gbit/s B2B OWC system, based on commercial components [35]. This OWC system was based on the D-LOS link architecture to maximize the received optical power while minimizing the power consumption. Notwithstanding, it had good tolerance to misalignment, so that it relied on precise mechanical mounting, i.e., with no need for an active alignment, which made it more robust to the vibrations of the rack [36]. The setup is sketched in Fig. 4. As optical source, it was selected a 1310 nm-VCSEL with 6 GHz bandwidth, 2 mW output power , and 16° emission angle. The laser was directly modulated by a 10 Gbit/s pseudo-random Non-Return-to-Zero (NRZ) electrical signal ($2^{15}-1$ pattern length) generated with a Pulse Pattern Generator (PPG). This produced a NRZ signal which, at the end of the link, was received by means of a OWC receiver a Positive-Intrinsic-Negative PD (PIN-PD) (9 GHz bandwidth and 50 µm active area). Its output was electrically amplified and analyzed using a Real-Time Oscilloscope (RTO) and, then, a Bit Error Ratio (BER)-tester. In front of TX and RX, two ball lenses were placed to control the beam divergence, optimize the transmission link, and improve the tolerance to the misalignment.

In preliminary characterization, the eye diagram of the 10 Gbit/s signal (Fig. 5a) was first measured on axis; then the tolerance to radial misalignment D was derived. Specifically, it

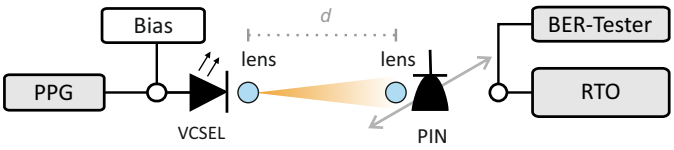

Fig. 4: Schematics of the B2B transmission setup for DCs. PPG: Pulse Pattern Generator; RTO: Real-Time Oscilloscope

This article has been accepted for publication in IEEE/OSA Journal of Lightwave Technology. This is the author's version which has not been fully edited and content may change prior to final publication. Citation information: DOI 10.1109/JLT.2025.3530819

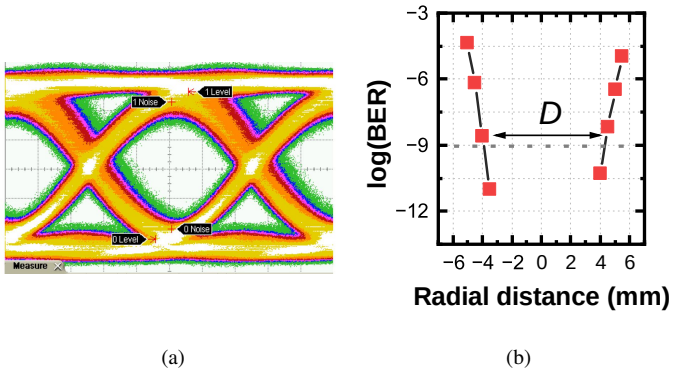

(a) (b)

Fig. 5: Eye diagrams of the 10 Gbit/s signal on-axis at 3 m (a) and measured BER values as a function of the radial distance from the optical axis (b) [35].

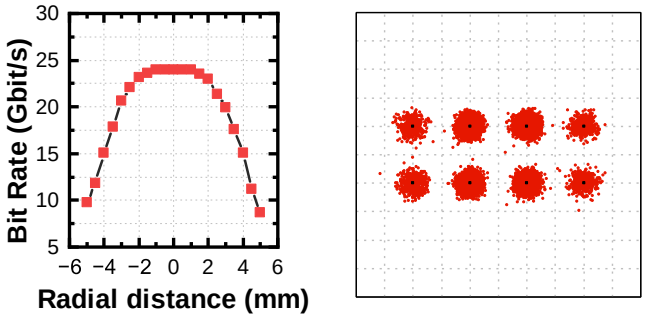

(a) (b)

Fig. 6: 24 Gbit/s experiment. Bit rate as a function of the radial misalignment (a) and constellations diagram of all the sub carriers taken with the RX on axis (radial distance equal to 0 mm) (b) [39].

was determined the value of the maximum radial displacement at which the BER was lower than 10^{-9}. To achieve this objective, the radial position of the RX was changed, and the BER was measured at each position. The results are reported in Fig. 5b and shown a D value of ± 4 mm, able to compensate moderate vibrations [36]. The power efficiency was measured to be around 10 pJ/bit. This was close to the target in DCs [37], although the setup was not optimized to minimize the power consumption.

The bit rate of this system was limited by the bandwidth of the optoelectronics devices. However, since the measured Signal to Noise Ratio (SNR) was high, the capacity could improve by using Discrete Multi-Tone (DMT) modulation. For this experiment, we chose DMT, since it is very frequently used in OWC, and has been shown to provide high-speed transmission. However, other modulation formats (e.g. PAM) could be considered and they might provide further improvements [38]. This allowed us to achieve a 24 Gbit/s link by maximizing the bit rate [39], fully exploiting the available SNR. In this experiment, the VCSEL was thus directly modulated by the DMT signal generated by a MATLAB script running on a PC and then fed to a Digital-to-Analog Converter (DAC). The DMT signal consisted of frames of 256 samples, with Hermitian symmetry and had a total electrical bandwidth of 6.5 GHz, with $N - 1 = 103$ active sub-carriers (frequency spacing of 62.5 MHz) and 4 times oversampling. After propagation, the electrical output was directed to an Analog-to-Digital Converter (ADC), which was then connected to a PC that carried out the BER measurement.

In Fig. 6a, we show the achievable bit rate as a function of the radial distance from the optical axis, given a fixed pre-Forward Error Correction (FEC) BER of 3.8×10^{-3}: noteworthy, the associated electronic processing of FEC introduces a delay negligible compared to the latency requirements in a DC. As expected, the radial misalignment remains a key parameter influencing the system functionality. The maximum bit rate was achieved on the optical axis and decreases symmetrically as the RX moves from the axis, reaching a bit rate of 10 Gbit/s at 6 mm distance. In Fig. 6b, we report the constellation diagrams of all the active subcarriers. Here, we can see superimposed the constellation values of 4-QAM and 8-QAM modulation formats in the case of no radial misalignment.

This system was further improved, eventually achieving the remarkable bit rate of 40 Gbit/s. To this aim, the optical source and the photo-detector bandwidths were optimized, replacing the previous source with a VCSEL having 8 GHz bandwidth and a InGaAs PIN-PD Photo-Diode (PD) having 13 GHz bandwidth. In this measurement, the signal wavelength was 1550 nm, at which the InGaAs PD shows a slightly higher responsivity (around 1 A/W). Here, the VCSEL was directly modulated by a DMT waveform made by 326 subcarriers covering a total bandwidth of around 10 GHz, with a carrier spacing of 30 MHz. After propagation, the electrical output was sent to an ADC, which was interfaced to the PC that analyzed the signal and finally performed the signal demodulation and the BER measurement.

Again, the radial misalignment affected the maximum achievable bit rate at any position. As shown in Fig. 7a, the maximum bit rate was achieved with no misalignment and decreased as the distance increased, going down to 27 Gbit/s at a 1 mm. For example, in Fig. 7b, we report the constellation diagrams of all DMT subcarriers symbols where a maximum modulation order of 32-QAM was reached.

IV. VCSEL SYSTEMS IN CHALLENGING ENVIRONMENTS

VCSEL-based OWC systems were also studied for various application scenarios that are characterized by extreme conditions, such as data transmission inside the spacecrafts and in HEP experiments. There, we can expect significant stress on the system and the optoelectronic devices in terms of mechanical vibrations, temperature fluctuations, and radiation exposure. In the following, we will review the final effect of these extreme conditions on the performance of the VCSEL sources and we leave the study of the degradation phenomena (such as oxide delamination or crack formation) to an accurate and dedicated device analysis [41].

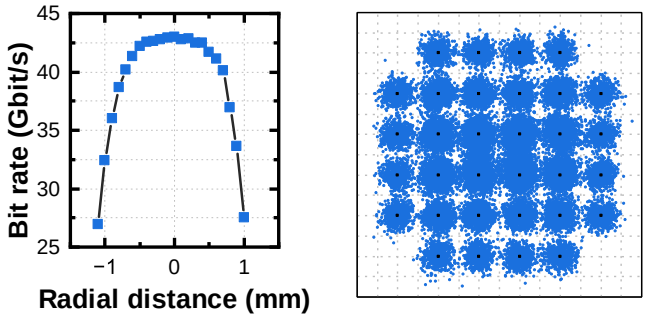

(a) (b)

Fig. 7: 40 Gbit/s experiment. Achieved bit rate vs the radial distance from the optical axis (a) and constellation diagram of all the subcarriers taken for perfect alignment (b) [40].

A. OWC System for short-distance space links

Wireless transmission in spacecraft is a key emerging area of interest for OWC, largely due to the considerable challenges posed by the harness of cabled communication systems in the design of satellites. This harness includes physical cables, connectors, and very bulky shielding to protect the wires from extreme external effects. As a result, it can represent up to 8% of the total mass of the satellite [42]. Moreover, during the Assembly Integration and Test (AIT) phase, the arrangement and tests of the cabled communications require precise and time-consuming operations. RF communications were proposed as an alternative to traditional cabled systems; however, they present issues due to their Electro-Magnetic Compatibility (EMC) with the equipment onboard the satellites: this prevents their use in satellites. Fiber-based solutions might be another viable alternative. However, despite the weight reduction due to optical fibers compared to copper cables, the incorporation of robust shielding results in a considerable mass increase; moreover, they would also ask for the same rigorous arrangement and testing procedures as any other physical cable.

Recent developments in intra-Spacecraft (intra-SC), AIT and extra-Spacecraft (extra-SC) OWC links demonstrated the feasibility of designing intra-satellite networks that can transfer data wirelessly, offering enhanced flexibility and lower costs. This requires OWC systems to adapt the bus signals commonly used for on-board communication to the free space. Among these buses, the MIL-STD-1553, which has a long track record, is still the most frequently used: we thus designed our OWC solutions to support this protocol.

The three mentioned scenarios (intra-SC, extra-SC, and AIT) have very different requirements in terms of OWC design, such as received optical power, link architecture, tolerance to ambient light, and misalignment. In particular, the extra-SC links should connect external elements (e.g., star tracker, advanced smart active antennas, deployable reflectors) to the outer hub, which is then connected by cables to the inner central unit. The OWC system can provide bidirectional data communication between the two TRXs, on the top plane of the satellite main body. In this scenario, a key impairment

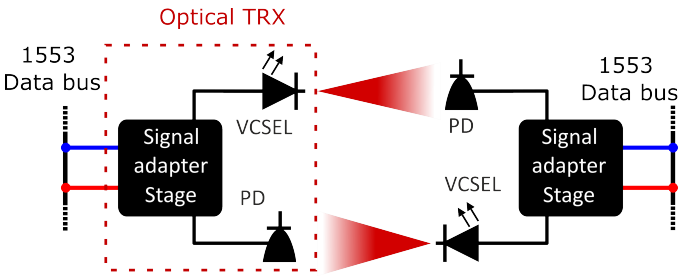

Fig. 8: Schematics of the extra-SC transmission setup.

can come from the strong background sunlight, which acts as noise. Therefore, to achieve the required SNR, the optical links require significant received power, which can be achieved only using the high beam directionality typical of VCSELs. This is not enough, as the link also requires a narrow optical filter (central wavelength at 850(2) nm and the FWHM equal to 10(2) nm) at the RX, which can only be compatible with a laser source. Therefore, VCSELs are the best suitable candidate sources in the optical TXs (noteworthy, in intra-SC and AIT links we rather can take advantage of LED- based TXs [10], [43]).

The demonstrated OWC system consisted of two identical optical TRXs that were designed as transparent interfaces between the MIL-STD-1553 and the bidirectional OWC transmission [44]. Each TRX includes a RX stage for the detection of the optical signal, an adaptation stage for converting the electrical MIL-STD-1553 signal into a format suitable for the OWC transmission, and a TX stage.

In the TX, it was chosen a VCSEL emitting at 850 nm (0.85 nm spectral width, 4° emission angle and 1 mW output power). The optical RX included a $5 \times 5\,\mathrm{mm}^2$ PIN-PD with the sensitivity range in the IR spectrum and a FoV of 70°. The 850 nm wavelength was chosen thanks to the availability of large-area photodetectors that are highly responsive at this wavelength and allow for high detection efficiency. The narrow emission angle of the VCSEL is a key parameter that, when coupled with the FoV of the received signal, allows the establishment of an optical wireless link that is resilient to sunlight conditions and exhibits robust tolerance to misalignment.

We note that, due to the D-LOS architecture, the two units of the system required an optical alignment, yet a good tolerance to the radial misalignment was also needed. Therefore, it has been measured the optical irradiance as a function of the transverse distance from the optical axis and measured the RX sensitivity ($-13\,\mathrm{dBm/cm}^2$). We note that this sensitivity value was obtained by emulating strong sunlight on the RX and it is 25 dB higher than the sensitivity in dark conditions. This allowed us to estimate the tolerance to misalignment, which was found to be around ±15 mm, as can be seen in Fig. 9. After the characterization, the bidirectional transmission of the MIL-STD-1553 between the two TRXs was successfully completed without any observed errors.

In space, another important area is the development of OWC systems for high-speed data transmission within short volumes. In particular, it was recently designed and realized another OWC system for Gbit/s transmission inside a 3U CubeSat,

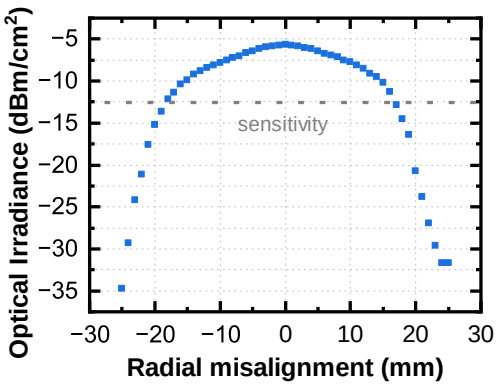

Fig. 9: Received optical power density as a function of radial misalignment. The red dashed line indicates the RX sensitivity when exposed to strong sunlight [44].

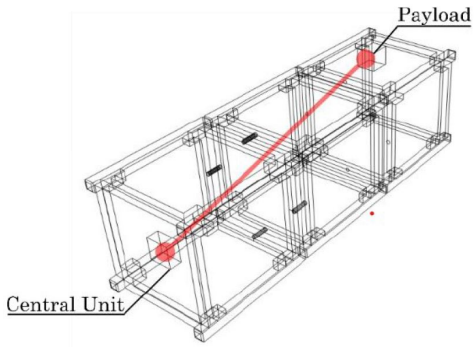

Fig. 10: Schematic of the OWC link inside the CubeSat

which is a new type of satellite, with a modular design (3U indicates that it is made of three unitary blocks) [45]. Here, the requirements were quite different because the system should have a high data rate although over a short distance. Clearly, we again chose a VCSEL as a TX exploiting a D-LOS link architecture. For this application, a 1 Gbit/s transmission was established between the central unit of the CubeSat and the payload placed at the other end of the volume, at 30 cm. The configuration is sketched in Fig. 10.

As for the extra-SC scenario, the tolerance of the OWC link against the misalignment was assessed by measuring the BER as a function of the position of the RX along the transversal X-axis. The results are reported in Fig. 11 and show a tolerance of ±2 mm, well above the mechanical precision of the satellite assembly.

It is important to highlight that, in this case, the behavior of the commercial optoelectronic components was assessed under mechanical, thermal, and radiation stress [46], [47]. Indeed, the typical qualifications required for space-grade components were carried out, to assess the tolerance of VCSEL and PD to space conditions. Various components were tested under strong mechanical stress, high-temperature variations, and intense X-ray irradiation [48].

The mechanical tests were conducted in a clean room (ISO 8 level). Here, VCSEL and PD were assembled on their

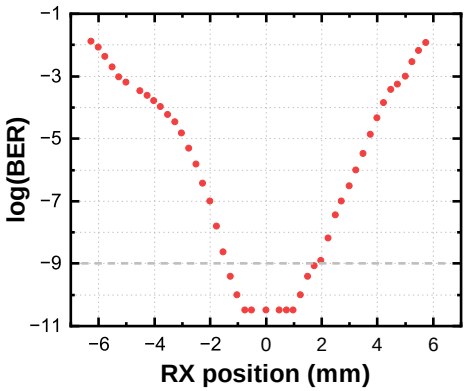

Fig. 11: BER as a function of the position of the RX along the X-axis.

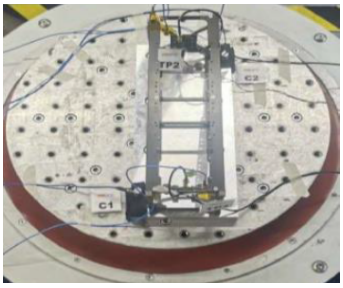

Fig. 12: The mockup of the CubeSat mounted on the vibrating platform [47].

boards and fixed to the CubeSat structure by specific interface plates and mounted on the vibrating platform. The devices then suffered the typical mechanical stresses occurring in a common type of launcher (SpaceX Falcon-9 type), similar to those of launchers suitable for the various types of CubeSats: the mechanical frequencies were between 1–1000 Hz with an acceleration between 0.5–2 G.

The IV curve of the VCSEL was measured before and after the mechanical test to assess the effect of vibrations. The results provide a voltage difference in the order of few mV, as reported in Fig. 13, indicating that the VCSEL was not significantly affected by the (strong) vibration.

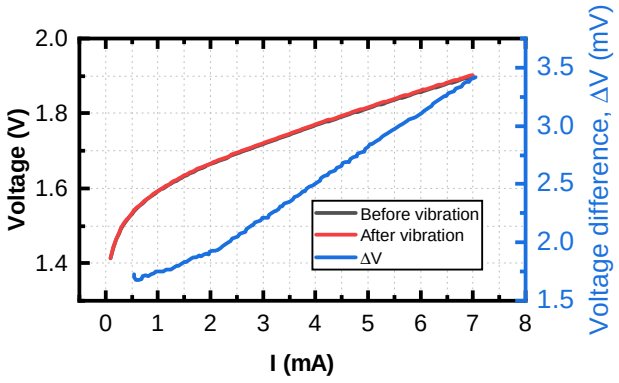

Fig. 13: IV curve of the VCSEL before and after the mechanical test.

This article has been accepted for publication in IEEE/OSA Journal of Lightwave Technology. This is the author's version which has not been fully edited and content may change prior to final publication. Citation information: DOI 10.1109/JLT.2025.3530819

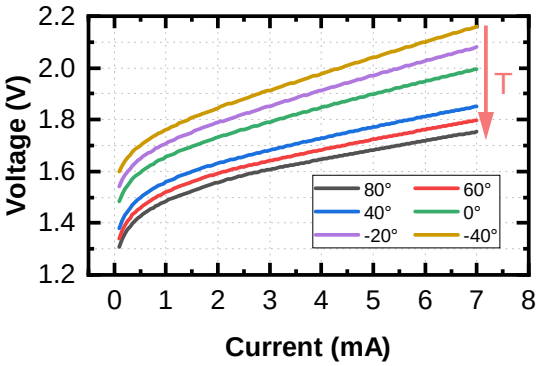

Fig. 14: Measured IV curve of the VCSEL at different temperature.

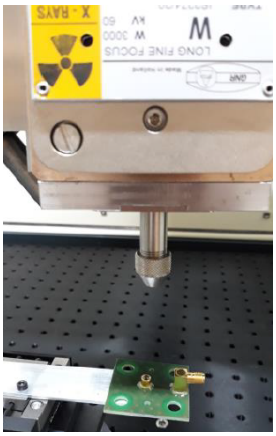

Fig. 15: Picture of the test of the VCSEL under the X-ray irradiation system [47].

In order to check the resistance to thermal variations, the VCSELs were then tested in a thermal chamber, where they experienced the typical temperature variations in a LEO satellite: –40–80 °C. The maximum rate of descent between one step and the next was chosen to be 3 °C/min and, for the thermalization of the structure, we waited 10 min after each step, after which the characteristics of the devices were checked. The IV curves are reported in Fig. 14. As expected from the theory of the pn junction (see also Section II), the temperature variations affected the device curve [27]–[29], although the VCSEL maintained a quite acceptable performance.

As the last test, the tolerance to irradiation was investigated: the VCSELs were irradiated with a typical dose of X-ray corresponding to 25 years at the LEO orbit. It can be estimated a dose of around 40 krad/yr, from which, in 25 years, we obtain a total dose equal to 1 Mrad. The VCSELs were placed under the X-rays source (Fig. 15) and subjected to 7 emissions of 10 minutes each with irradiation of 14.5 krad/min. At regular intervals of 10 minutes, the VCSEL were tested by taking the complete IV curve.

As reported in Fig. 16, no noticeable variation was observed in the characteristics of the VCSEL.

Due to severe practical limitations in the setup, during the tests it was not possible to carry out some specific measurements (such as optical power and BER) and we could just measure the I-V curve. However, this is an excellent indicator for evaluating the proper operation of a VCSEL transmitter. We should also note that in this first analysis, we focused on the effects of external factors on the individual device and will leave to future investigations the effect of extreme conditions on the whole communication system.

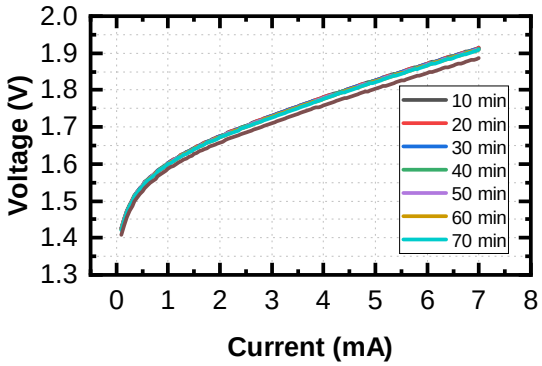

Fig. 16: IV curve of the VCSEL at different temperature.

B. OWC System for High Energy Physics

Another peculiar field that can benefit from the use of VCSEL-based OWC systems is HEP. As an example of this type of application, let us consider the Compact Muon Solenoid (CMS) experiment at the Large Hadron Collider (LHC), where high-energy particles are generated and collide. Huge systems of detectors are deployed to track the effects of the collisions: namely, large-scale detection facilities are based on a significant number of silicon strips and silicon pixel detectors, arranged in concentric circles [49], [50].

Presently, this requires over 40 000 optical fiber links for the analog readout and digital control channels [51]. This large amount of connections and components asks for a high material budget and determines space limitations as well as great issues related to cable installation and maintenance. Wireless links could be a valid alternative to optical fiber, however, when a 60 GHz RF signal was considered to transmit high speed data, it showed significant practical issues [52].

It is clear that OWC can be a complementary solution in these HEP experiments. A schematic representation of a possible configuration is shown in Fig. 17, where B2B OWC could allow data transmission among boards in adjacent circles. In this frame, a 10 Gbit/s OWC system was realized, having a 20 cm link distance and 3 mm misalignment tolerance , which could optically connect the neighbor layers of the detector boards in the CMS tracker [53]. Especially in the inner circles, the VCSELs are expected to suffer from huge irradiation of X-rays and heavy particles (e.g. protons). They were thus tested against very high-dose irradiation.

For these tests, a 1310 nm VCSEL with output power up to 2 mW and a PIN-PD with an active area of 50 µm and a 3 dB

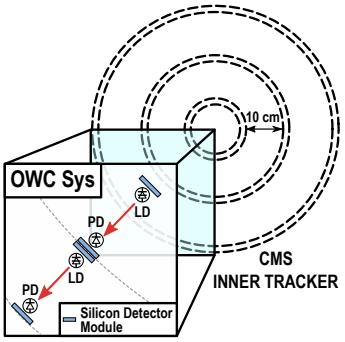

Fig. 17: Scenario of an OWC system in the CMS inner tracker, showing concentric circles of detectors; the inset shows the proposed B2B links among detector boards on the same radial direction.

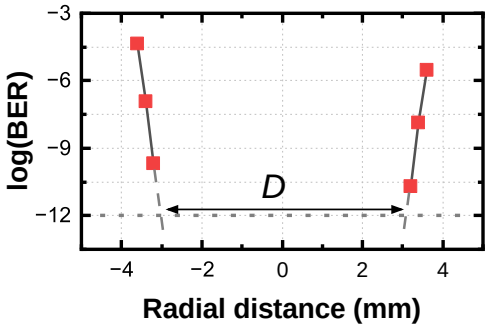

Fig. 18: Measured BER values as a function of the radial distance from the optical axis [53].

bandwidth of 12 GHz were selected. We chose to work in this wavelength region mainly because there are available VCSELs and PD that are suitable for free-space applications and meet the bandwidth requirement of the system.

The transmission setup is similar to the one depicted in Fig. 4. A current source and a PPG were used to drive the VCSEL with a 10 Gbit/s NRZ signal (Pseudo-Random Binary Sequence (PRBS), $2^{31}-1$ bits). After propagation, the optical signal was received by the PD and analyzed using a BER tester and a RTO. VCSEL and PD were placed at 20 cm distance, using a ball lens in front of each of them, to improve the beam collimation at the TX and the light focusing at the RX.

A first transmission test was carried out with the TX and the RX perfectly aligned. After that, the measurement was repeated by displacing the RX with respect to TX along the radial axis, perpendicularly to the optical axis. At each position, the BER value was measured to assess the tolerance of the system to the misalignment. As shown in Fig. 18, a tolerance of ± 3 mm was obtained, which is largely lower than expected mechanical tolerances in the real arrangement of the detector boards (± 1 mm).

After demonstrating the transmission, the OWC system compatibility was evaluated with HEP experiments, testing the optoelectronic components at the CERN proton Irradiation facility (IRRAD). The optical components selected for the assessment were two types of VCSELs with different emission wavelengths: 1310 nm and 1550 nm, mounted on three boards. The boards were placed in the irradiation chamber at -21 °C and exposed to a protons beam with 5×5 mm^2 spot size and intensity of 4×10^{11} p/(cm^2 spill) at 24 GeV of beam momentum. The proton irradiation lasted 24 hours.

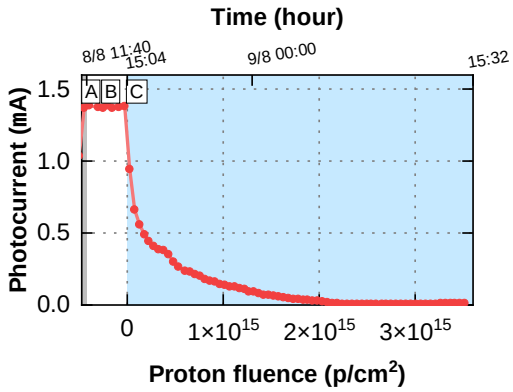

Fig. 19: Measured photocurrent from the PD placed in front of the VCSEL as a function of proton fluence and time. Different colored areas indicate Area A: cooling ramp; Area B: idle; Area C: p-beam ON [53].

In Fig. 19, we report the optical power of one of the boards as received by the external photodiode, as a function of the proton dose (time). All other boards exhibit similar behavior. Area A represents the cooling ramp phase to reach an equilibrium temperature of -21 °C, which lasted for 30 min. The emitted optical power of the VCSELs increased at lower temperatures, as expected from the datasheet. Area B indicates an idle phase of about 3 hours; after that, the boards were exposed to the proton beam for 24 h (represented by area C). As expected, the performance of the VCSEL decreases exponentially as the number of irradiated protons increased. Unfortunately, they cannot survive to the target final proton flux. However, we can see that the tested VCSELs can tolerate a total proton fluence of around 10^{14} p/cm^2: this indicates that they could be suitable in other experimental conditions, with lower proton-irradiation conditions. As an example, they could be placed in the outer region of the concentric detector system, where the proton density is much lower.

A comparable OWC system was developed and its performance under X-ray irradiation was evaluated. The devices were placed at 14 mm under the X-rays source with a dose rate of 10.8 Mrad/hour. The irradiation was continuous for 22 hours, with a total dose of 238 Mrad; during the tests, the bias current, the received power, and the forward voltage, were measured at regular intervals (15 min). We highlight that these conditions are by far more severe than those previously assumed for the CubeSat (presented in Section IV-A), due to the much higher dose expected in the CMS experiments. Additionally, the VCSELs used in the two tests have different materials and wavelengths; therefore, any direct comparison between the two X-rays results would not be fair.

The experimental results are shown in Fig. 20, where we reported the LI (Fig. 20a) and IV (Fig. 20b) curves of the VCSEL under test in three different conditions: before (black) and after (red) irradiation. We only observed a slight change

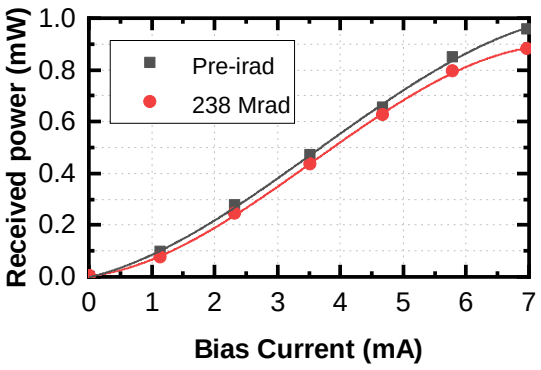

(a)

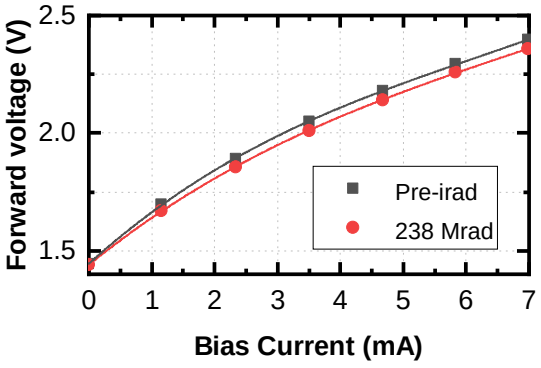

(b)

Fig. 20: L-I curve (a) and I-V curve (b) of the VCSEL under X-rays [54].

in the LI slope. However, this variation was negligible and did not affect the performance of the OWC system. This variation was probably a consequence of the increased temperature of the optical source, which was not under control. No relevant change in the threshold current and the IV curve was observed. This indicates that even huge X-ray irradiations do not affect the VCSEL functionality.

V. Conclusion

In this paper, we presented several new OWC system solutions that were recently designed, realized, and tested to be used in new and distinct application areas (high-energy physics, DCs data transmission, and intra-satellites communication). In all of them, the peculiar features of VCSELs played a key role in reaching the expected performance. These OWC systems can allow establishing wireless links on significant distances, up to 3 m, and achieve very high data rates, up to 40 Gbit/s.

Since the user environments are not the usual indoor office/home, they can have extreme conditions; therefore some of those VCSELs were tested to withstand the key stressing phenomena that can be found in space or during HEP experiments (strong accelerations, high-temperature variations, and X-ray and proton irradiation). The obtained results indicate that VCSELs sources are quite robust in these stressing conditions. This clearly indicates that VCSELs can be successfully used in these applications, thus the corresponding OWC systems represent a valid alternative to cabled systems and wireless RF systems.

Furthermore, they can be employed to address some emerging issues associated with these scenarios. In this framework, developing VCSEL-based OWC solutions can bring clear advantages, as they facilitate wireless communication, removing the need for cables. Depending on the scenario, this could give significant benefits in terms of reduced complexity, lower occupied volume, and possibly lower costs of installation and maintenance. In some cases, this could also prove an energy-efficient alternative to other wireless connections.

Finally, we should note that the recent advancements in VCSEL technology [33] indicate a promising potential for future deployment in other new and different areas, suggesting that there are still intriguing opportunities and applications that could be explored in the future.

References

[1] M. Uysal and H. Nouri, "Optical wireless communications — An emerging technology," in *2014 16th International Conference on Transparent Optical Networks (ICTON)*, 2014, pp. 1–7.

[2] M. Z. Chowdhury *et al.*, "Optical Wireless Hybrid Networks: Trends, Opportunities, Challenges, and Research Directions," *IEEE Communications Surveys & Tutorials*, vol. 22, no. 2, pp. 930–966, 2020.

[3] A. Al-Kinani *et al.*, "Optical Wireless Communication Channel Measurements and Models," *IEEE Communications Surveys & Tutorials*, vol. 20, no. 3, pp. 1939–1962, 2018.

[4] Z. Ghassemlooy *et al.*, "Emerging Optical Wireless Communications-Advances and Challenges," *IEEE Journal on Selected Areas in Communications*, vol. 33, no. 9, pp. 1738–1749, 2015.

[5] S. Dittmeier *et al.*, "Wireless data transmission for high energy physics applications," *EPJ Web Conf.*, vol. 150, p. 00002, 2017.

[6] N. Karafolas *et al.*, "Optical communications in space," in *2009 International Conference on Optical Network Design and Modeling*, 2009, pp. 1–6.

[7] G. Cossu *et al.*, "Bi-directional 400 Mbit/s LED-based optical wireless communication for non-directed line-of-sight transmission," in *OFC 2014*. IEEE, 2014, pp. 1–3.

[8] P. Brandl *et al.*, "OWC using a fully integrated optical receiver with large-diameter APD," *IEEE photonics technology letters*, vol. 27, no. 5, pp. 482–485, 2014.

[9] N. Saha *et al.*, "Survey on optical camera communications: challenges and opportunities," *IET Optoelectronics*, vol. 9, no. 5, pp. 172–183, 2015.

[10] G. Cossu *et al.*, "Demonstrating Intra-Spacecraft Optical Wireless Links," *IEEE Access*, vol. 11, pp. 30 920–30 928, 2023.

[11] D. Mahgerefteh and C. Thompson, "Techno-economic Comparison of Silicon Photonics and Multimode VCSELs," in *Optical Fiber Communication Conference*. Optica Publishing Group, 2015, p. M3B.2.

[12] J. K. Guenter *et al.*, "Commercialization of Honeywell's VCSEL technology: further developments," in *Vertical-Cavity Surface-Emitting Lasers V*, K. D. Choquette and C. Lei, Eds., vol. 4286, International Society for Optics and Photonics. SPIE, 2001, pp. 1 – 14.

[13] G. Schaefer, "28Gbit/s VCSEL Reliability Report," VI Systems GmbH, Tech. Rep., 2014.

[14] A. Maharry *et al.*, "A 50 Gbps 9.5 pJ/bit VCSEL-based Optical Link," in *2021 IEEE Photonics Conference (IPC)*, 2021, pp. 1–2.

[15] A. Jaffal *et al.*, "VCSELs market outlook in consumer sensing and data communication," in *Vertical-Cavity Surface-Emitting Lasers XXVIII*, C. Lei and K. D. Choquette, Eds., vol. 12904, International Society for Optics and Photonics. SPIE, 2024, p. 1290409.

[16] Yole Intelligence, "VCSEL–Market and Technology Trends 2022," Tech. Rep., 2022.

[17] P. Westbergh *et al.*, "850 nm VCSEL operating error-free at 40 Gbit/s," in *22nd IEEE International Semiconductor Laser Conference*, 2010, pp. 154–155.

[18] H.-T. Cheng *et al.*, "Recent Advances in 850 nm VCSELs for High-Speed Interconnects," *Photonics*, vol. 9, no. 2, 2022.

[19] Y.-C. Chang and L. A. Coldren, "Efficient, high-data-rate, tapered oxide-aperture vertical-cavity surface-emitting lasers," *IEEE Journal of Selected Topics in Quantum Electronics*, vol. 15, no. 3, pp. 704–715, 2009.

[20] T. Anan *et al.*, "High-speed 1.1-μ-range ingaas vcsels," in *OFC/NFOEC 2008 - 2008 Conference on Optical Fiber Communication/National Fiber Optic Engineers Conference*, 2008, pp. 1–3.

[21] J. He *et al.*, "Design of a PAM-4 VCSEL-Based Transceiver Front-End for Beyond-400G Short-Reach Optical Interconnects," *IEEE Transactions on Circuits and Systems I: Regular Papers*, vol. 69, no. 11, pp. 4345–4357, 2022.

[22] D. Kuchta *et al.*, "An 800 Gb/s, 16 channel, VCSEL-based, co-packaged transceiver with fast laser sparing," in *2022 European Conference on Optical Communication (ECOC)*, 2022, pp. 1–4.

[23] M. R. Murty *et al.*, "Toward 200g per lane vcsel-based multimode links," in *2024 Optical Fiber Communications Conference and Exhibition (OFC)*, 2024, pp. 1–3.

[24] H. Soda *et al.*, "GaInAsP/InP Surface Emitting Injection Lasers," *Japanese Journal of Applied Physics*, vol. 18, no. 12, p. 2329, dec 1979.

[25] K. Iga, "Surface-emitting laser-its birth and generation of new optoelectronics field," *IEEE Journal of Selected Topics in Quantum Electronics*, vol. 6, no. 6, pp. 1201–1215, 2000.

[26] ——, "VCSEL: born small and grown big," in *Vertical External Cavity Surface Emitting Lasers (VECSELs) X*, J. E. Hastie, Ed., vol. 11263, International Society for Optics and Photonics. SPIE, 2020, p. 1126302.

[27] A. Larsson, "Advances in VCSELs for Communication and Sensing," *IEEE Journal of Selected Topics in Quantum Electronics*, vol. 17, no. 6, pp. 1552–1567, Nov. 2011.

[28] P. Moser, *VCSEL Fundamentals*. Cham: Springer International Publishing, 2016, pp. 13–44.

[29] F. Koyama, "Recent Advances of VCSEL Photonics," *Journal of Lightwave Technology*, vol. 24, no. 12, pp. 4502–4513, 2006.

[30] E. P. Haglund *et al.*, "Impact of Damping on High-Speed Large Signal VCSEL Dynamics," *Journal of Lightwave Technology*, vol. 33, no. 4, pp. 795–801, 2015.

[31] L. Coldren, S. Corzine, and M. Mashanovitch, *Diode Lasers and Photonic Integrated Circuits*, ser. Wiley Series in Microwave and Optical Engineering. Wiley, 2012.

[32] R. Olshansky *et al.*, "Frequency response of 1. 3. mu. m InGaAsP high speed semiconductor lasers," *IEEE J. Quant. Electron.; (United States)*, vol. QE-23:9, 9 1987.

[33] N. Haghighi *et al.*, "19-Element 2D Top-Emitting VCSEL Arrays," *J. Lightwave Technol.*, vol. 39, no. 1, pp. 186–192, Jan 2021.

[34] IEC, "Iec62471:2006 "photobiological safety of lampsand lamp systems"," Jul. 2006.

[35] W. Ali *et al.*, "10 Gbit/s OWC System for Intra-Data Centers Links," *IEEE Photonics Technology Letters*, vol. 31, no. 11, pp. 805–808, 2019.

[36] M. Curran *et al.*, "Handling rack vibrations in FSO-based data center architectures," in *2018 International Conference on Optical Network Design and Modeling (ONDM)*, 2018, pp. 47–52.

[37] C. Kachris, K. Kanonakis, and I. Tomkos, "Optical interconnection networks in data centers: recent trends and future challenges," *IEEE Communications Magazine*, vol. 51, no. 9, pp. 39–45, 2013.

[38] S. Hranilovic, *Wireless optical communication systems*. Springer Science & Business Media, 2006.

[39] G. Cossu *et al.*, "VCSEL-Based 24 Gbit/s OWC Board-to-Board System," *IEEE Communications Letters*, vol. 23, no. 9, pp. 1564–1567, 2019.

[40] G. Cossu *et al.*, "High-speed optical wireless links for datacenters," in *Metro and Data Center Optical Networks and Short-Reach Links III*, A. K. Srivastava, M. Glick, and Y. Akasaka, Eds., vol. 11308, International Society for Optics and Photonics. SPIE, 2020, p. 1130804.

[41] Y. Zhang and J. Zhao, "Analysis of common failure causes in oxide VCSELs," in *International Conference on Optoelectronic Materials and Devices (ICOMD 2021)*, Y. Lu, Y. Gu, and S. Chen, Eds., vol. 12164, International Society for Optics and Photonics. SPIE, 2022, p. 121641H.

[42] R. Amini *et al.*, "New generations of spacecraft data handling systems: Less harness, more reliability," in *57th International Astronautical Congress*, Valencia, Spain, Oct. 2006.

[43] L. Gilli *et al.*, "Optical Wireless Communication in an Avionics Test Facility for Spacecrafts," *IEEE Sensors Journal*, vol. 24, no. 6, pp. 8982–8990, 2024.

[44] G. Cossu *et al.*, "Optical Wireless Links for Extra-Spacecraft Communication," *IEEE Aerospace and Electronic Systems Magazine*, vol. 39, no. 4, pp. 42–48, 2024.

[45] S. Song, H. Kim, and Y.-K. Chang, "Design and implementation of 3u cubesat platform architecture," *International Journal of Aerospace Engineering*, vol. 2018, no. 1, p. 2079219, 2018.

[46] E. Ertunc *et al.*, "Preliminary study on diffuse OWC for intra-CubeSat Communication," in *2020 Italian Conference on Optics and Photonics (ICOP)*, 2020, pp. 1–3.

[47] N. Vincenti *et al.*, "Testing a 1 Gbit/s Optical WIreless Communication System against Extreme Space Conditions," in *International Conference on Wireless for Space and Extreme Environments - WISEE 2023*, 2023.

[48] G. Cossu *et al.*, "High-speed optical wireless system for extreme space conditions," *IEEE Journal of Radio Frequency Identification*, pp. 1–1, 2024.

[49] V. Karimäki, "The CMS tracker system project: Technical Design Report," 1997.

[50] "The CMS tracker: addendum to the Technical Design Report," 2000.

[51] J. Troska *et al.*, "CMS optical links: Lessons learned from mass production," in *12th Workshop on Electronics for LHC and Future Experiments (LECC 2006)*, 9 2006, pp. 529–533.

[52] D. Pelikan *et al.*, "Radial transfer of tracking data with wireless links," 01 2014.

[53] A. Messa *et al.*, "Optical Wireless Systems for High Energy Physics: Design and Characterization," in *2019 21st International Conference on Transparent Optical Networks (ICTON)*, 2019, pp. 1–4.

[54] W. Ali *et al.*, "Design and Assessment of a 2.5-Gb/s Optical Wireless Transmission System for High Energy Physics," *IEEE Photonics Journal*, vol. 9, no. 5, pp. 1–8, 2017.